Title: Effect of Dilution on Reaction Properties and Bonds Formed Using Mechanically Processed Dilute Thermite Foils

Authors and Affiliations

Alex H. Kinsey[1*], Kyle Slusarski[1], Karsten Woll[2], David Gibbins[1], Timothy P. Weihs[1]

1. Johns Hopkins University, Department of Materials Science and Engineering, 3400 North Charles St., Baltimore, MD 21218
2. Karlshruhe Institute of Technology (KIT), Institute for Applied Materials (IAM), 76344 Eggenstein-Leopoldshafen, Germany

*Corresponding author. akinsey3@jhu.edu, (410) 516-2023

Author email addresses: kaslusarski@gmail.com, karsten.woll@kit.edu, jgibbins6@gmail.com, weihs@jhu.edu

Abstract

Thermites have been used for over a century for joining applications and in this paper we present fully-dense diluted thermite foils that react in a self-propagating manner and produce sufficient heat and molten braze to join aluminum, magnesium, and iron-based alloys. Al:NiO, Al:CuO, and Al:Cu_2O thermite systems were systematically diluted with Ni or Cu to decrease the maximum reaction temperature and hence the amount of gas generated during the self-propagating reactions. Velocities and mass ejection were measured for reactions within free-standing foils as a function of dilution. The dilution that leads to quenching during propagation within a bond is identified and finally, Al:NiO:10wt%Ni and Al:CuO:40wt%Cu foils were used to demonstrate the ability to join aluminum, magnesium, and iron-based alloys.

Keywords

Thermites; Exothermic Brazing; Mechanical Processing; Bonding, Self-propagation

Introduction

For over 100 years the thermite process has been used to join metal components together by exothermically reacting powder mixtures to create molten metal[1]. In 1895, Dr. Hans Goldschmidt patented the process whereby aluminum reduces iron oxide to produce molten iron[2]. The thermite reaction is an oxidation-reduction reaction; a fuel reduces a metallic oxide, producing molten metal, the oxidized fuel, and heat:

$$A + MO = AO + M + \Delta H \quad (1)$$

A is the fuel, in our case aluminum, M is the reduced metal, and ΔH is the heat of reaction.

Thermite reactions have found many uses[1, 3], including lining ceramic pipes[4, 5], and synthesizing composites[6]. Typical thermite reaction processes for joining applications, such as joining railroads or electrical connections, involve a crucible and a mold[7, 8]. The thermite mixture is placed into the crucible and ignited, the molten metal then flows, usually by force of gravity, into the joint area. The resulting oxide from the reaction, being less dense than the molten metal, remains outside of the joint interface and can be removed easily. This technique, however, does not work for certain applications, such as joining sheets of metal, where flowing molten metal into a narrow gap between two sheets is not viable. For these types of joints, furnace brazing or other area joining techniques, such as adhesive joining, are preferred.

Free-standing multilayer reactive foils made by sputter deposition of aluminum and nickel multilayers have been used to join metals[9–12], ceramics[13, 14], and metallic glasses[15–17]; this form of reactive bonding can easily be scaled to large areas bonds. These foils have been commercialized as NanoFoil® and their use in joining applications has been named the NanoBond® process. The process uses an exothermic intermetallic formation reaction as a localized heat source to solder or braze components. Additional solder is required and added as a prewet layer on the surface, or as a freestanding solder/braze foil; often a metallization layer must also be used to promote adhesion to the bonding component[10, 12]. The strength of these bonds has been found to depend on the strength of solder that is used [14]. The fast nature of the self-propagating reaction and localization of the heat limits thermal degradation of the components being bonded [18], allowing heat sensitive materials and devices to be joined together without thermal damage.

With respect to joining, redox or thermite reactions offer two significant advantages compared to intermetallic formation reactions. First, the higher reaction temperatures of the redox reactions make them more capable of enabling brazing of components. Second, the molten metal produced by the redox reaction can act as a filler (braze) material, thereby eliminating the need for pre-existing solder or braze on the components being bonded. It is anticipated that these advantages of the redox reactions have the potential to broaden the range of joining applications that can be addressed with reactive foils acting as local heat sources.

Due to their highly exothermic nature, however, thermite reactions can generate substantial amounts of vapor[3]. Maximum reaction temperatures can exceed the boiling points of the products and reactants, thereby producing gaseous species. Such gas generation is detrimental to joint fabrication[19], as it can cause material ejection, creating pores and voids in the resulting braze, thereby limiting the strength of the bond. As a result, reducing the gas production of thermite foils is necessary to ensure a strong, pore-free bond. It has been shown that diluting thermites, or changing the stoichiometry, can have a significant effect on the reactivity of the reaction. For example, diluting with excess inert product (oxide) can reduce the reaction temperature and gas production[20–22]. Some diluents can also enhance the reactivity of the system either due to the intermetallic reactions that occur before the onset of the thermite reaction[23] or due to enhanced thermal conductivity from the chosen diluent[24].

The present study contributes to the expansion of exothermic brazing via the utilization of the thermite-based reactive foils. In detail, we use our recently introduced Redox Foils[25] that are fully dense thermite foils produced by mechanical powder processing, and explore key parameters relevant for joining. Al:NiO, Al:CuO, and Al:Cu_2O are used as the thermite systems. Diluents are chosen so as to increase the amount of molten metal or braze that is generated during the reaction. Hence, we choose elemental Ni and Cu as diluents. Reaction velocities, mass ejection, and reactivity are quantified, and the stoichiometry of the foils is systematically altered to lower the adiabatic temperature below the boiling points of all product and reactant species in order to minimize gas production during their self-sustaining exothermic reactions. Finally, two diluted thermite chemistries were selected to demonstrate the ability to join Al 6061, Mg AZ 31 and hot stamped boron steel.

Experimental Procedures

Materials Fabrication

Redox Foils were fabricated by processing the micron-sized powders that are listed in Table 1. Powder sizes were measured using a Horiba LA-950V2 Particle Size Distribution Analyzer with powders suspended in either water or isopropyl alcohol; D10, D50, and D90 values are also reported in Table 1. These powders were mixed manually in 10 g batches according to the desired thermite chemistry and the desired dilution with excess Cu or Ni. The mass percent of diluent is defined relative to the mass of the total powder mixture, and the remaining mass is composed of the thermite mixture in the stoichiometric ratio as given in Table 2. Each thermite stoichiometry was fabricated with dilutions that ranged from 0wt% to 40wt% in increments of 10wt%.

Material	Supplier	Size	Purity	D10 (μm)	D50 (μm)	D90 (μm)
Al	Alfa Aesar	-325 mesh	99.5%	10.4	16.9	28.6
NiO	Alfa Aesar	-325 mesh	99%	8.0	13.4	21.8
CuO	Alfa Aesar	-325 mesh	97%	5.6	8.9	13.7
Cu_2O	Sigma Aldrich	<5 micron	97%	3.3	5.5	8.7
Cu	Alfa Aesar	-325 mesh, 10%+325	99%	15.9	27.0	45.8
Ni	Alfa Aesar	-325 mesh	99.8%	7.9	15.4	37.5

Table 1: Powders used for fabrication of Redox Foils with size and purity as quoted by manufacturer; the measured D10, D50, and D90 values for the powders are also reported

Thermite System
$2Al + 3CuO + xCu \rightarrow Al_2O_3 + (3+x)Cu$
$2Al + 3Cu_2O + xCu \rightarrow Al_2O_3 + (6+x)Cu$
$2Al + 3NiO + xNi \rightarrow Al_2O_3 + (3+x)Ni$
$2Al + 3NiO + xCu \rightarrow Al_2O_3 + 3Ni + xCu$

Table 2: Stoichiometric ratios for thermites used in this work where x represents the amount of dilution. In this paper, dilution is reported as a mass percent of the entire mixture.

After powders were mixed in small batches, they were pressed into a tube for swaging and rolling. Each batch of powder was pressed into a carbon steel tube by applying 40 MPa of pressure using an Instron 5582 load frame equipped with a 50 kN load cell; 3 to 4 batches of powder were incorporated into each tube. Working with small batches helps to minimize particle segregation during fabrication and ensure a uniform chemistry distribution throughout the tube and within the resulting Redox Foil. The steel tubes have a 15 mm outer diameter and a 1.5 mm wall thickness. One end of the steel tube was plugged with an aluminum rod prior to adding powders, and another was pressed into the tube after the powders were added. The aluminum rods act to contain the powders and make sure that the powders deform during the subsequent mechanical processing.

The tubes were swaged using a 3F Fenn Rotary Swager in 13 steps until the final outer diameter of the tube was 3.17 mm. After swaging, the resulting cylinder was cut and cold rolled using a 3" rolling mill and 200 μm reductions in thickness until the flattened rod was approximately 1 mm thick. Additional 100 μm reductions were also enabled via cold rolling until the desired thickness was achieved. After rolling, the Redox Foil was removed from the steel jacket by filing away the sides of the jacket and peeling off the top and bottom sections. Final thicknesses of the Redox Foil ranged from 375 to 475 μm. Images of samples during various stages of the swaging and rolling process are shown in Figure 1(a).

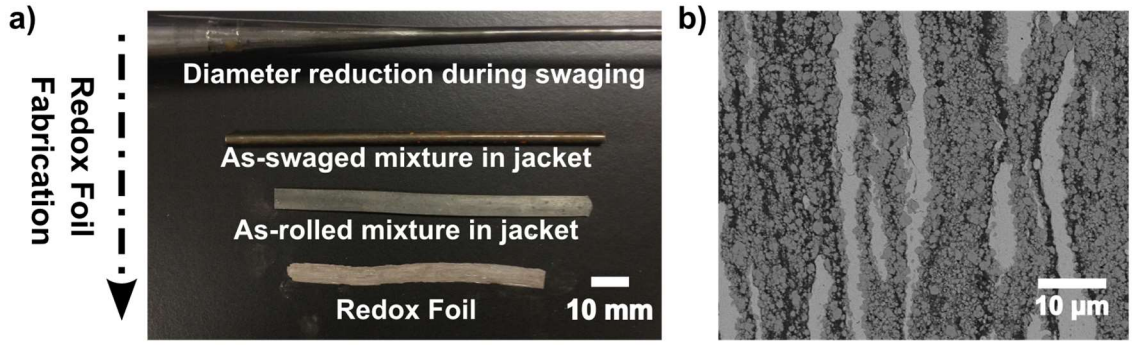

Figure 1: a) A photograph showing samples from the various stages of the Redox Foil fabrication process. The radial reductions during swaging produce a 3.17mm diameter tube that is then rolled flat. Once the steel is removed the Redox Foil is exposed. b) A SEM micrograph of Al:NiO:30wt%Ni showing the microstructure of a typical Redox Foil. The lightest color is the nickel diluent, the gray is nickel oxide, and the dark gray or black is aluminum.

Experimental Procedures

The velocity of self-propagating thermite reactions of Redox Foils was determined using two different methods. The first employs a series of optical fibers at known distances that capture the light emitted from the propagating reaction, as explained previously[26]. The second uses a NAC Memrecam HX-6 High Speed Camera. All velocity measurements were obtained with a foil resting on a ceramic block and clamped at one end to fix the position of the foil and prevent any translational motion due to the gas generated by the reaction. Reactions were ignited with a spark on the unclamped side of the foil, and both measurement techniques yielded similar values, all of which are reported here. Three tests per chemistry were performed and the error bars represent one standard deviation.

Variations in mass ejection with dilution and thermite chemistry were determined by measuring the mass of particulates and vapor that were captured on 0.18 mm thick steel shims measuring 2.5 x 2.5 cm, supported 2.5 cm above the Redox Foil during reaction. The steel coupon was weighed before and after the reaction and the change in mass is attributed to the particles and vapor from the reaction that deposit on the shim. Like the velocity tests, three samples trials were performed for each chemistry.

Differential scanning calorimetry was performed with a Perkin Elmer DSC 8000 using 7 to 10 mg of material per scan. Each specimen was heated twice to 725 °C at 40 C/min in with argon at 40 ml/min. The first scan captured the power released by the irreversible phase transformations within the reaction. The second scan provided a baseline to account for the heat capacity of the reacted sample and the crucible. The power measured in the second scan was subtracted from the power measured in the first scan in order to determine heat released by the reaction.

To identify whether the diluted thermite reactions could propagate between two components being bonded, 3.17 mm thick samples of Aluminum 6061-T6 and Magnesium AZ31B were cut with a wire EDM to final dimensions of 12.7 mm x 6.35 mm. The bonding surfaces, those exposed to the Redox Foil, were polished with 320 and 600 grit SiC paper

followed by an acetone and ethanol rinse to create uniformly rough but clean surfaces. Redox Foils were cut to dimensions as depicted in Figure 2, placed between the bonding components and a load of 400 N was applied with an Imada manual stand equipped with a DPS-110R Digital Force Gauge. Once position and loaded, foils were ignited by an electrical spark outside of the bond area as depicted in Figure 2.

Bonding experiments were performed with samples of Aluminum 6061-T6, hot stamped boron steel (HSB), and Magnesium AZ31B that were 1.25 mm thick. Samples were cleaned with an ethanol and acetone wash but were not polished, except for the Mg AZ31, which was polished to 600 grit in order to be of similar thickness to other alloys tested. The setup for bonding specimens was the same as the quenching setup in Figure 2 except the dimensions of the metallic samples were twice as long, measuring 24.5 mm x 6.35 mm. Once bonded the single lap shear specimens were tested in tension using an Instron 5582 load frame at a rate of 0.1 mm/min.

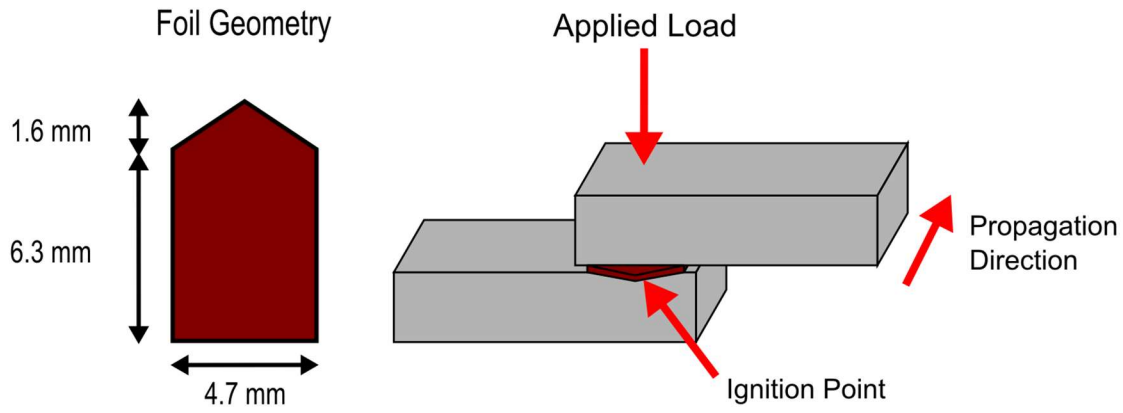

Figure 2: A schematic of the geometry for quenching tests and bonding. Redox Foils were cut to the proper size and placed between the two bonding components. Reactions in the foils were ignited outside of the bond area and propagated between the components that were under 400 N of force.

Results

Velocity and Mass Ejection

The velocities of reactions in the Al:NiO:Ni and the Al:Cu_2O:Cu systems decrease by over an order of magnitude as dilution increases from 0 to 40 wt.%, as shown in Figure 3(a). However, the type of diluent does play a role. Note that when the Al:NiO system is diluted with Cu instead of Ni reaction velocities do not drop as rapidly with 10 or 20 wt.% dilution. For 30 wt.% dilution of the Al:NiO system with Cu there is a substantial drop in reaction velocity but the Al:NiO:Cu foils continue to propagate faster than the Al:NiO:Ni foils for the same dilution; at 40wt% Cu dilution, however, the propagation velocity drops below that of 40wt% Ni dilution. In contrast to the Al:NiO and Al:Cu_2O systems, the velocities of reactions in the Al:CuO:Cu system remain relatively constant between 1 and 2 m/s for the same range of dilution (0 to 40 wt.%).

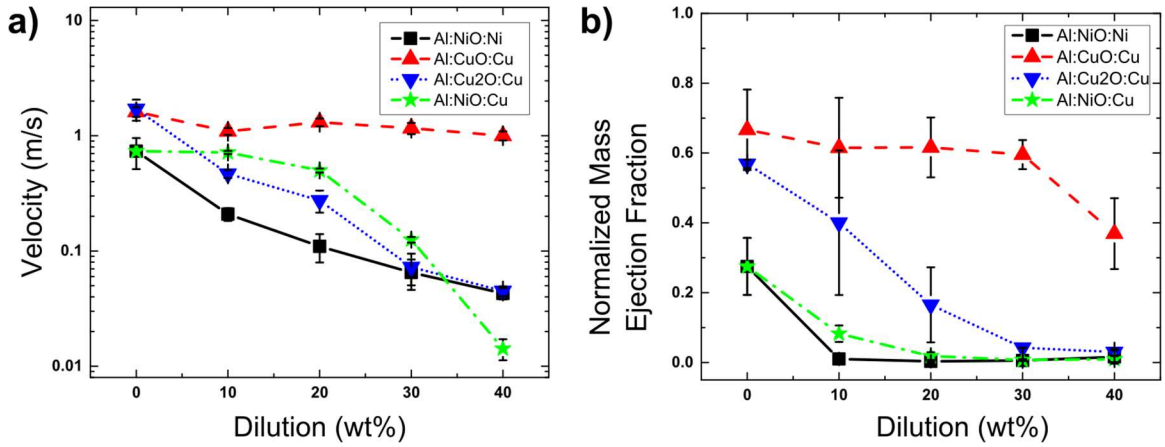

Figure 3: a) Velocities measured for self-propagating reactions in Redox Foils as a function of wt.% dilution and dilution chemistry. b) The normalized mass ejection as a function of the volume percent of braze (metal) in the final reacted product, assuming no loss of braze material. The weight percent dilutions for each set of samples have been added next to the data points for clarity.

The amount of material that is ejected as the thermite reactions self-propagate is summarized in Figure 3(b) for the same set of samples and similar trends are observed. Mass ejection from the Al:NiO and Al:Cu_2O Redox Foils shows a strong dependence on the amount of dilution, similar to reaction velocities, and there is some dependence on the chemistry of the dilution for the Al:NiO system. Dilution with Cu instead of Ni leads to more mass ejection for 10 and 20 wt.% dilutions in Al:NiO foils. However, independent of diluent, the Al:NiO system ejects less mass, compared to the Al:Cu_2O system. In contrast to both the Al:NiO and Al:Cu_2O systems, the Al:CuO system ejects significant mass for all dilutions and the amount of ejection decreases little with dilution until 40 wt.% of excess Cu is added. For the Al:CuO foils at least 60% of their mass is ejected until the 40 wt.% Cu dilution is reached.

DSC

Low temperature reactions were characterized using DSC to understand the effect of dilution on how heat is released. DSC traces for Al:NiO:Ni, Al:CuO:Cu, and Al:Cu_2O:Cu are displayed in Figure 4. For all chemistries studied, increasing the amount of dilution decreased the magnitude of the exothermic peaks, indicating that less heat is generated by the reactions on a per gram basis. The temperature of the exothermic peaks does not shift with increased dilution. This indicates that adding diluent does not substantially increase the spacing between the two reactants, the fuel and the oxide, as seen in earlier studies [27].

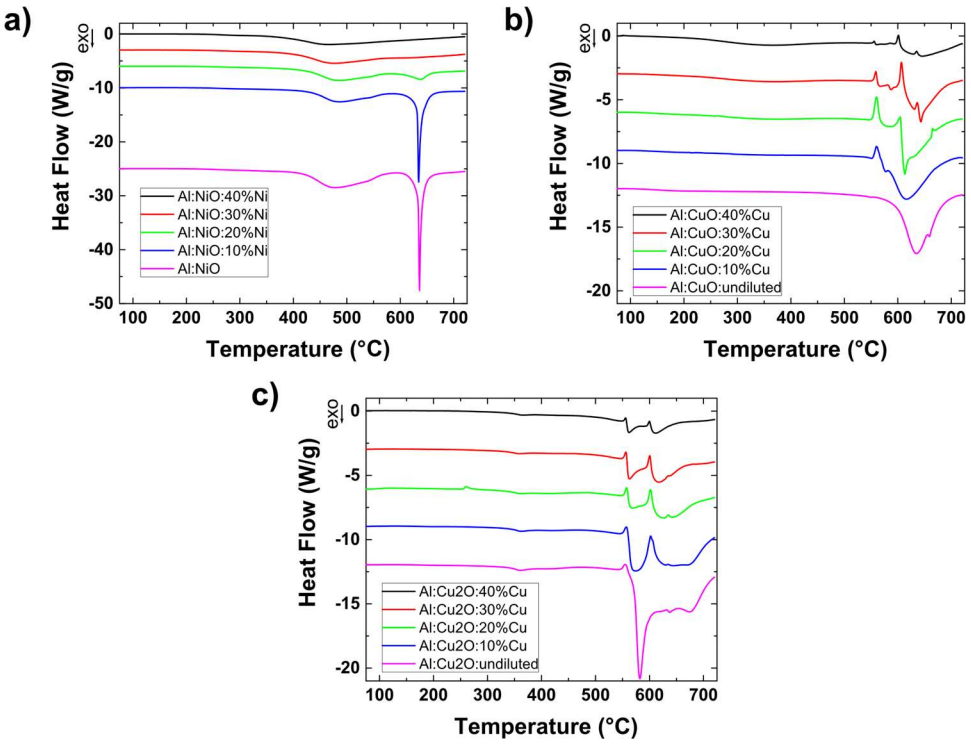

Figure 4: DSC traces as a function of dilution are presented for three systems a)Al:NiO:Ni b) Al:CuO:Cu, and c) Al:Cu_2O:Cu. For comparison the individual DSC traces are shifted along the 7-axis.

Similar DSC characterization was performed on Al:NiO:Cu with 10 and 20 wt.% dilutions to characterize the reactivity of the samples and to help understand why velocity in the Al:NiO system increases when the Ni diluent is replaced with Cu (Figure 3(a)). For all DSC traces in Figure 5 the first peak, which occurs around 450 °C, corresponds to the formation of $NiAl_3$ and Ni_2Al_3 intermetallics, as determined from previous work [25]. This first exotherm is suppressed when diluting with Cu because there is less Ni in the system to enable formation of Al-Ni intermetallics, and because the presence of Cu at the Al/NiO interfaces hinders Ni diffusion into Al. The second exotherm, which is enabled by the melting of the aluminum fuel and its subsequent rapid reaction with other components, is shifted to lower temperatures for both the 10 and 20 wt.% dilutions of Cu in contrast to Ni. The peak of the exotherm shifts from 633 °C for Al:NiO:10%Ni to 551 °C for Al:NiO:10%Cu and shifts from 637 °C for Al:NiO:20%Ni to 561 °C for Al:NiO:20%Cu. We attribute both shifts to a lowering of Al's melting temperature due to the Al being alloyed with Cu in addition to Ni.

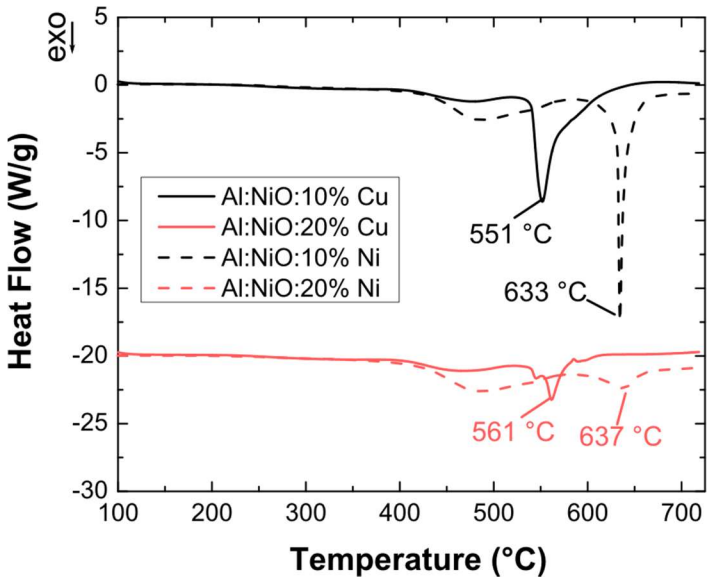

Figure 5: Heat flow data recorded for DSC scans of Al:NiO samples diluted with copper and nickel. Dotted lines are diluted with nickel and solid lines are diluted with copper. The second exotherm shifts to a lower temperature for copper diluted samples. 20 wt.% diluted samples are offset for clarity.

Quenching and Bonding

Given the reaction velocities reported in Figure 3(a) were characterized using free-standing foils, we performed additional experiments to determine which samples can self-propagate through a bond interface. As shown in Figure 2 we ignited foils outside a bond interface and determined whether or not reactions could self-propagate across the bond area. When reactions quenched, they typically did so as soon as their reaction front reached the edge of bonding material. However, in a few cases the reactions propagated into the bond area before quenching as demonstrated in Figure 6. (In compiling data for Figure 5(d) we labeled a reaction as being quenched whether it stopped propagating at the edge of the bond area or within the bond area.) The quenching results in Figure 6(d) correlate with the velocities measurements and mass ejection results in Figure 3. The Al:CuO:Cu foils with the fastest reactions and the most mass ejection yielded reactions that propagated across the full bonding area for both Mg AZ31 and Al 6061 components, and for all dilutions. In contrast, reactions in the Al:NiO:Ni foils quenched in the bonding configuration when 20 wt.% Ni was added, but quenched at a higher dilution of 30wt.% when Cu was added and the samples were reacted between Mg AZ31. Similar trends were observed with reactions in the Al:Cu-$_2$O:Cu system; the foils quenched between Mg AZ31 components for 20 wt.% Cu and between the more thermally conductive Al 6061 components at 10 wt.% Cu. Based on these dilution limits for quenching and based on measurements of mass ejection, Al:NiO:10%Ni and Al:CuO:40%Cu foils were chosen to bond metallic components and bond strengths are summarized in Figure 7.

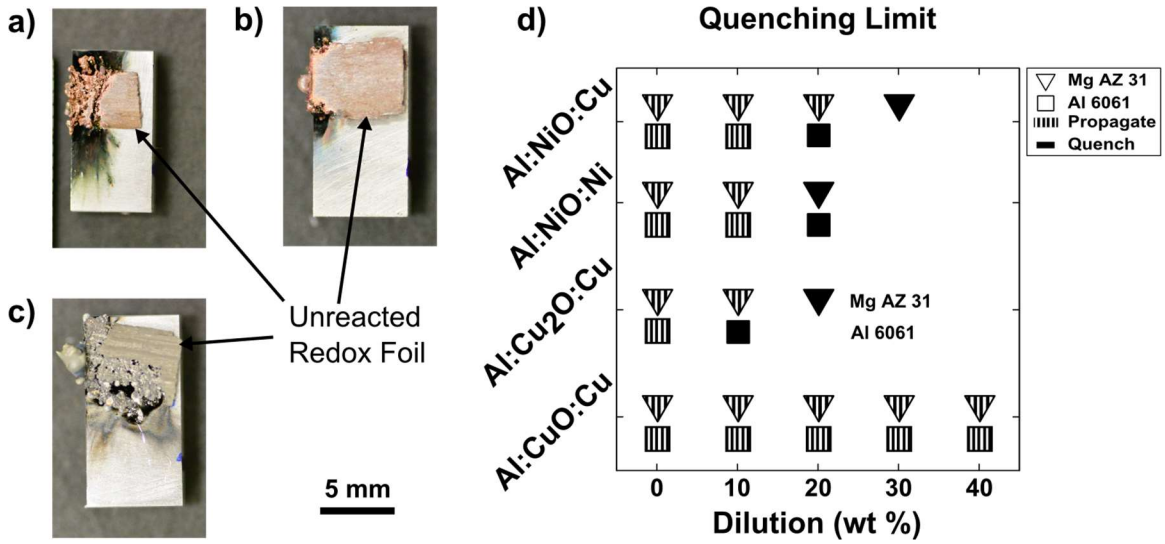

Figure 6: Images of Redox Foils in which reactions quenched on various components: a) Al:Cu_2O:10%Cu on Al 6061 b) Al:Cu_2O:20%Cu on Mg AZ 31 c) Al:NiO:20%Ni on Al 6061. d) An overview of quenching tests indicating dilution limits for bonding configurations for the four Redox Foil systems.

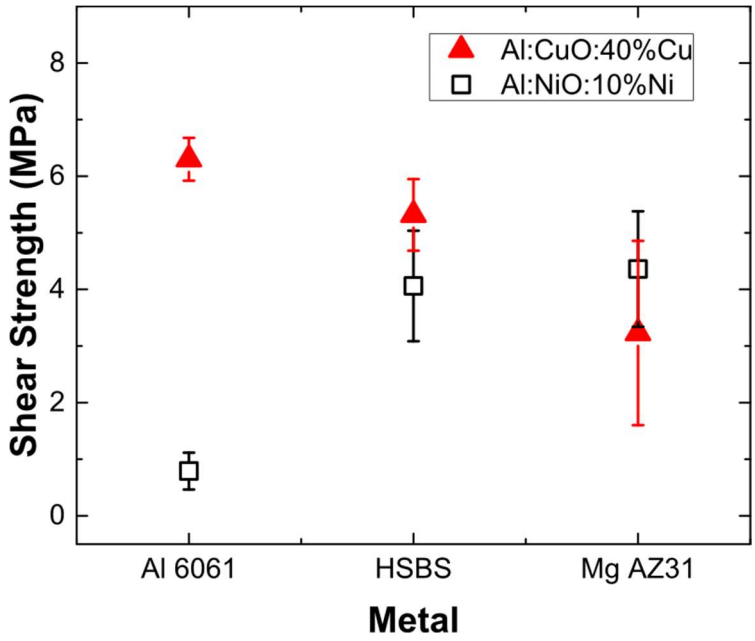

Figure 7: Shear strengths for three different components and two Redox Foils. The error bars represent standard deviations from multiple tests.

Discussion

As seen in Figure 3 diluting thermite-based materials with excess metal can reduce both reaction velocities and mass ejection significantly. We attribute these reductions primarily to a lowering of the adiabatic flame temperatures for the reactions, based on earlier efforts [25]and theoretical calculations (Figure 8). A lower adiabatic or maximum temperature

due to dilution will slow atomic intermixing and this in turn will decrease reaction velocities. Relatively strong decreases in velocity are seen in Figure 3(a) when the Al:NiO system is diluted with Ni and the Al:Cu_2O system is diluted with Cu. These velocity reductions correlate well with the decreases in the calculated adiabatic temperatures with dilution that are seen in Figure 8 for the same foils. The adiabatic temperature drops smoothly for both systems after relatively low levels of dilution are reached. However, if the adiabatic temperature is pinned to a distinct phase change, such as the boiling of Cu, dilution may need to reach a critical level before the maximum temperature actually decreases and velocities drop sharply. Such is the case for the Al:CuO system diluted with Cu. The calculated adiabatic temperature does not drop below the boiling point of Cu until more than 50 wt.% excess Cu is added (Figure 8). Thus, one would anticipate only limited drops in maximum temperatures and reaction velocities in the Al:CuO system when diluting up to 40 wt.% Cu as seen in Figure 3(a).

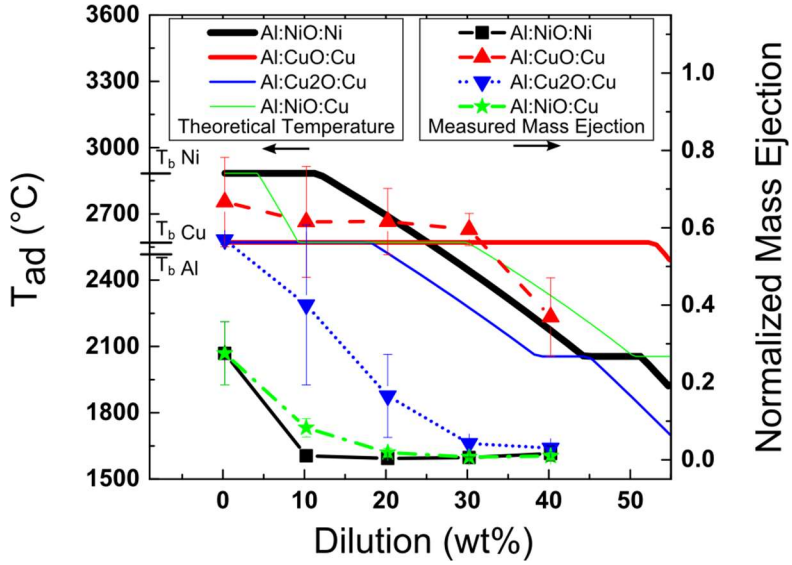

Figure 8: The calculated adiabatic temperature and normalized mass ejection for a given weight percent dilution. The solid lines are the calculated adiabatic temperatures (right axis) and solid points, connected with dashed lines, are measured mass ejection (left axis), previously plotted as function of volume percent in Figure 3(b).

Like the reaction velocities, decreases in mass ejection also correlate well with drops in the calculated adiabatic temperatures as shown in Figure 8. Once temperatures drop below the boiling point for Ni or Cu, less gas is generated and fewer particles are blown off the foils. This general correlation is seen for all samples. As the calculated adiabatic flame temperature decreases below the boiling point of Ni or Cu, mass ejection falls to nearly zero for Al:NiO:Ni. This is also true for the Al:NiO samples that are diluted with Cu. The correlation also holds for the Al:Cu_2O samples but some additional dilution appears necessary to reach nearly zero normalized mass loss. In these samples, some localized hot spots may exist which could lead to mass ejection, either from vaporization of the products

or fracturing of particles. Internal porosity in the sample or loosely attached particles near the surface of the foils could also cause some minimal mass ejection.

In addition to boiling of Cu or Ni, mass ejection can also be caused by oxide reduction and the formation of gaseous oxygen. Many researchers have found that in Al:CuO thermite reactions, the CuO decomposes to Cu_2O and O_2 during the reaction[28, 29]. This production of O_2 gas could lead to local pockets of pressure and subsequent expulsion of particles from the foil. Not only will this generation of O_2 lead to mass loss, it can also promote reaction velocities in certain cases. When reaction velocities are measured in burn tube experiments, energy can be transferred ahead of the reaction front via convection from the hot gases [30] and by advection of reacted molten material [31]. However, these forms of energy transfer are reduced to due to the effects of dilution in the freestanding velocity case, and essentially eliminated in quenching/bonding experiments where the foils are constrained by the bonding components.

As a final comparison of reaction properties relative to the amount of dilution, we note that when an Al:CuO sample diluted with 40 wt.% Cu reacts completely it produces approximately 63% Cu by volume, similar to an undiluted Al:Cu_2O sample (Figure 3(b)). In addition, both samples have similar reaction velocities (Figure 3(a)). This suggests that the relative amount of Al, Cu and O in the as-processed samples has a large influence on reaction properties. The slightly higher reaction velocity and mass ejection for the undiluted Al:Cu_2O samples is attributed to the fact that there is no barrier separating the oxide from the aluminum fuel in the Cu_2O case. In contrast, for the diluted Al:CuO system, the elemental copper impedes diffusion of oxygen from the oxide to the aluminum fuel and slows reaction velocities, likely reducing the maximum temperature and mass ejection.

Beyond the amount of diluent that is added, the chemistry of the diluent can impact reaction properties in multiple ways, as seen for the Al:NiO system diluted with both Ni and Cu. First, by adding excess Cu instead of excess Ni, the adiabatic temperature of the reaction is pinned to the boiling point of Cu and more diluent is required to reduce mass ejection to zero as seen in Figures 3(b) and 7. Second, because copper has a higher thermal conductivity than nickel (401 W/m K versus 90.7 W/m K [32]), heat travels along the Cu-diluted Al:NiO Redox Foil faster than the Ni-diluted foils and reaction velocities are higher, as seen in Figure 3(a). Similar results were reported by Shen et al.[24] who found that adding small amounts of silver nanoparticles to Al:CuO composites enhanced combustion velocities. However, after substantial dilution, the velocity can decrease significantly when too much heat gets drawn into the diluent and decreases the rate of heat production. This occurs in the Al:NiO:40%Cu case where reaction velocity substantially drops below the velocity of the Al:NiO:40%Ni.

The third impact of diluent chemistry relates to melting temperatures and their impact on reaction velocities. As seen in the DSC scans in Figure 4(a), the Al:NiO:Ni samples have large second exotherms slightly below the melting temperature of Al. The exothermic nature of the second reaction is attributed to the melting of the Al fuel and its rapid oxidation in a molten state. Thus, the lower the melting temperature, due to alloying of the Al by Ni or Cu, the earlier the mixing is enhanced and the sooner heat is released. When the Al:NiO system

is diluted with Cu instead of Ni, the second exotherm shifts to lower temperatures (Figure 5) because the Al-Cu system has a lower eutectic temperature, than the Al-Ni system. We argue that this lower melting temperature for the Al fuel when diluted with Cu will enhance the oxidation of the Al, and hence the rate of heat production and the resulting reaction velocities. This hypothesis is supported by our high speed video observations that the self-propagating reactions progress primarily in a condensed state, and reaction rates are controlled by mass diffusion, as many other researchers have reported for other thermite systems and microstructures[33–38]. Thus, the higher reaction velocities of Al:NiO foils when diluted with Cu instead of Ni can be explained in part by a lowering of Al's melting temperature. Similar arguments were posed by Marin et al. who found that depositing thin Cu layers between Al and CuO layers in sputtered multilayer films enhanced reactivity and flame propagation speeds [39].

Given the fact that adding diluents to minimize gas production also slows the self-propagating reactions, highly diluted foils are more susceptible to quenching in a bonding configuration. Slower reaction speeds provide more time for heat to dissipate into the surrounding components, which cools and slows the reactions further[40]. The data in Figure 6(d) demonstrates this effect. The reaction of an Al:Cu_2O Redox Foils with a 20 wt.% Cu dilution can propagate between two Mg AZ31 components but not between two Al 6061 components. Al 6061 has a higher thermal conductivity (167 W/m K)[41] compared to Mg AZ31 (100 W/m K)[42] and thus draws heat from the reaction faster than the Mg AZ31 components and thereby enables quenching. To enable propagation of these foils with higher levels of dilution, reactivity must be enhanced by decreasing the average spacing of the reactants within the Redox Foils without initiating partial reaction during foil fabrication. An alternative might be to separate the fuel from the diluent by the utilization of diluent-oxidizer core-shell geometries. By doing so the formation of less reactive diluent/fuel interfaces is avoided. In those mixtures, more reactive fuel/oxidizer interfaces are formed. We recently demonstrated this approach for the Al:NiO:Ni system and reported positive effects on velocity when Ni is added as Ni-NiO core-shell particles.[25]

Using the data in Figure 6(d) we chose Al:CuO foils with a 40 wt.% Cu dilution and Al:NiO foils with a 10 wt.% Ni dilution to enable bonding of three different components: Al 6061, Mg AZ31, and High Strength Boron Steel (HSB). Even though the Al:CuO foils with 40 wt.% dilution of Cu eject approximately 40% of their mass during self-propagation in a free-standing geometry, according to our relative measurement, they still enable bonding. In comparison, the Al:NiO foils with a 10 wt.% dilution of Ni eject essentially 0% of their mass during self-propagation in a free-standing geometry. Average shear lap strengths range from 1 to 6.5 MPa. Part of the success in joining can be attributed to the fact that mass ejection is inhibited during bond, because the components being bonded restrain particle ejection and reduce evaporation by lowering reaction temperatures. Based on multiple observations, material loss is restricted mainly to the edges of both Redox Foils. However, mass ejection and gas production do occur and create both small and large voids across the resulting composite interface layers.

Despite the fact that Al:CuO foils eject significant mass when they self-propagate, joints produced with these foils produce stronger bonds than the Al:NiO:10%Ni foils when bonding Al 6061 and HSB. The discrepancies in bond strength are attributed to differences in final product ratios and wetting characteristics. The products of the Al:CuO:40%Cu foils are 62.5% Cu by volume (assuming no loss of material due to ejection or vaporization), while the products of the Al:NiO:10%Ni foils are only 47.4% Ni by volume, the rest of the products being alumina. With more molten braze, the Al:CuO are more likely to enable bonding. The more important difference, though, is the fact that the molten Cu wets the components more readily than the molten Ni. Bonds made with Al:CuO:40%Cu foils fracture within the interface or braze layer, while bonds made with the Al:NiO:10%Ni foils fracture at the braze/component interface, indicating poor adhesion between the Ni braze and either one of the three components. This suggests that the molten Cu braze material can wet the bonding components more effectively than the molten Ni braze material and that the wetting characteristics of the molten braze are critical to the formation of strong bonds. Undertaking various additional surface treatments to remove native oxides, oils, and grit from the surfaces more effectively may also improve wetting for any of the braze materials.

For the Mg AZ31 joints, the bond strengths are similar for both the Al:NiO:10%Ni and the Al:CuO:40%Cu foils, but there is evidence of significant melting and potential vaporization of the Mg AZ31 surface during the reaction. Examination of the fracture surfaces displays pitting caused by the melting of the surface. This type of behavior is not seen in the Al 6061 and HSB bonds. For the steel bonds, the melting point is sufficiently high that the reaction does not cause melting. In the aluminum case, the high thermal conductivity transfers heat away from the bonding surface so rapidly that significant melting of the Al alloy is avoided. This result suggests that reducing the temperature profile seen by the surface of the Mg AZ31 should decrease the degree of melting of the Mg surface and may improve bond strengths.

Conclusions

We have demonstrated the ability to fabricate fully dense Redox Foils using Al:NiO, Al:CuO and Al:Cu_2O chemistries, and we have shown that one can tailor the reaction properties of the thermite mixtures by diluting with excess metal. With dilutions ranging from 0 to 40 wt.%, the excess metal decreases the propagation velocity as well as the mass ejected during propagation in a free-standing geometry. Some of the most heavily diluted foils, however, are unable to propagate across a bond interface due to heat losses to the components being bonded. In order to achieve bonding with more highly diluted foils, the average reactant spacing within the foils must be refined and/or the diluent chemistry must be optimized to speed heat generation within the foils. Using Al:NiO and Al:CuO Redox Foils we have shown an ability to bond Al, Mg and Fe-based alloys. Further refinement of the reactive foil and tailoring the wetting characteristics of the braze to the components being bonded should increase the strength of the resulting bonds.

Acknowledgements

We would like to thank Jordan Theriault and Evan Krumheuer for their assistance in performing the metallic bonds. This work was supported by the Department of Energy through their Vehicle Transportation Program and Award DE-EE0006441. K.W. acknowledges the support by the Robert Bosch Stiftung. TPW is an inventor of a related technology that has been licensed by Johns Hopkins University.

Conflict of Interest

The authors declare that they have no conflict of interest

References

1. Wang LL, Munir ZA, Maximov YM (1993) Review Thermite reactions: their utilization in the synthesis and processing of materials. J Mater Sci 28:3693–3708.
2. Goldschmidt H (1895) Verfahren zur Herstellung von Metallen oder Metalloiden oder Legierungen derselben.
3. Fischer SH, Grubelich MC (1998) Theoretical energy release of thermites, intermetallics, and combustible metals. 24th Int Pyrotech Semin. doi: 10.2172/658208
4. Mu L, Yin S, Yanping W, Heyi L (1997) The characteristics of combustion in a centrifugal-thermite process. J Mater Sci 32:4711–4713. doi: 10.1023/A:1018666511189
5. Odawara O, Ikeuchi J (1986) Vacuum Centrifugal-Thermite Process for Producing Ceramic-Lined Pipes. J Am Ceram Soc 69:C–85–C–86.
6. Reddy BSB, Das K, Das S (2007) A review on the synthesis of in situ aluminum based composites by thermal, mechanical and mechanical–thermal activation of chemical reactions. J Mater Sci 42:9366–9378. doi: 10.1007/s10853-007-1827-z
7. Lee FT (2006) Managing Thermite Weld Qualilty for Railroads. Weld J 85:24.
8. Schroeder LC, Poirier DR (1984) The mechanical properties of thermite welds in premium alloy rails. Mater Sci Eng 63:1–21. doi: 10.1016/0025-5416(84)90159-9
9. Duckham A, Spey SJ, Wang J, et al. (2004) Reactive nanostructured foil used as a heat source for joining titanium. J Appl Phys 96:2336. doi: 10.1063/1.1769097
10. Wang J, Besnoin E, Knio OM, Weihs TP (2005) Effects of physical properties of components on reactive nanolayer joining. J Appl Phys 97:114307. doi: 10.1063/1.1915540
11. Wang J, Besnoin E, Knio OM, Weihs TP (2004) Investigating the effect of applied pressure on reactive multilayer foil joining. Acta Mater 52:5265–5274. doi: 10.1016/j.actamat.2004.07.012
12. Wang J, Besnoin E, Duckham a., et al. (2003) Room-temperature soldering with nanostructured foils. Appl Phys Lett 83:3987. doi: 10.1063/1.1623943

13. Duckham A, Brown M, Besnoin E, et al. (2004) Metallic bonding of ceramic armor using reactive multilayer foils. Ceram. Eng. Sci. Proc. pp 597–603

14. Duckham a., Levin J, Weihs TP (2006) Soldering and Brazing Metals to Ceramics at Room Temperature Using a Novel Nanotechnology. Adv Sci Technol 45:1578–1587. doi: 10.4028/www.scientific.net/AST.45.1578

15. Swiston AJ, Hufnagel TC, Weihs TP (2003) Joining bulk metallic glass using reactive multilayer foils. Scr Mater 48:1575–1580. doi: 10.1016/S1359-6462(03)00164-7

16. Swiston AJ, Besnoin E, Duckham A, et al. (2005) Thermal and microstructural effects of welding metallic glasses by self-propagating reactions in multilayer foils. Acta Mater 53:3713–3719. doi: 10.1016/j.actamat.2005.04.030

17. Trenkle JC, Weihs TP, Hufnagel TC (2008) Fracture toughness of bulk metallic glass welds made using nanostructured reactive multilayer foils. Scr Mater 58:315–318. doi: 10.1016/j.scriptamat.2007.09.060

18. Duckham A (2006) Applying Localized Heat for Brazing and Soldering. Weld J 44–46.

19. Bahrami Motlagh E, Vahdati Khaki J, Haddad Sabzevar M (2012) Welding of aluminum alloys through thermite like reactions in Al–CuO–Ni system. Mater Chem Phys 133:757–763. doi: 10.1016/j.matchemphys.2012.01.086

20. Strunina AG, Ermakov VI, Averson ÉA (1979) Limiting conditions of ignition of gasless systems by a combustion wave. Combust Explos Shock Waves 15:484–489. doi: 10.1007/BF00743124

21. Dvoryankin A V, Strunina AG, Merzhanov AG (1985) Stability of combustion in thermite systems. Combust Explos Shock Waves 21:421–425. doi: 10.1007/BF01463412

22. Malchi JY, Yetter R a., Foley TJ, Son SF (2008) The Effect of Added Al 2 O 3 on the Propagation Behavior of an Al/CuO Nanoscale Thermite. Combust Sci Technol 180:1278–1294. doi: 10.1080/00102200802049471

23. Gheybi Hashemabad S, Ando T (2015) Ignition characteristics of hybrid Al–Ni–Fe2O3 and Al–Ni–CuO reactive composites fabricated by ultrasonic powder consolidation. Combust Flame 162:1144–1152. doi: 10.1016/j.combustflame.2014.10.006

24. Shen J, Qiao Z, Zhang K, et al. (2014) Effects of nano-Ag on the combustion process of Al–CuO metastable intermolecular composite. Appl Therm Eng 62:732–737. doi: 10.1016/j.applthermaleng.2013.10.039

25. Woll K, Gibbins JD, Slusarski K, et al. The utlilization of metla/metal oxide core-shell powders to enhance the reactivity of diluted thermite mixtures. Combust Flame. doi: 10.1016/j.combustflame.2016.02.006

26. Reiss ME, Esber CM, Van Heerden D, et al. (1999) Self-propagating formation reactions in Nb/Si multilayers. Mater Sci Eng A 261:217–222. doi: 10.1016/S0921-5093(98)01069-7

27. Knepper R, Snyder MR, Fritz G, et al. (2009) Effect of varying bilayer spacing distribution on reaction heat and velocity in reactive Al/Ni multilayers. J Appl Phys 105:083504. doi: 10.1063/1.3087490

28. Jian G, Chowdhury S, Sullivan K, Zachariah MR (2013) Nanothermite reactions: Is gas

phase oxygen generation from the oxygen carrier an essential prerequisite to ignition? Combust Flame 160:432–437. doi: 10.1016/j.combustflame.2012.09.009

29. Weismiller MR, Lee JG, Yetter R a. (2011) Temperature measurements of Al containing nano-thermite reactions using multi-wavelength pyrometry. Proc Combust Inst 33:1933–1940. doi: 10.1016/j.proci.2010.06.094

30. Sullivan KT, Kuntz JD, Gash a. E (2012) Electrophoretic deposition and mechanistic studies of nano-Al/CuO thermites. J Appl Phys 112:024316. doi: 10.1063/1.4737464

31. Egan GC, Zachariah MR (2015) Commentary on the heat transfer mechanisms controlling propagation in nanothermites. Combust Flame 162:2959–2961. doi: 10.1016/j.combustflame.2015.04.013

32. Lide DR (2015) CRC Handbook of Chemistry and Physics, 96th Edition 2015-2016. www.hbcpnetbase.com.

33. Jacob RJ, Jian G, Guerieri PM, Zachariah MR (2015) Energy release pathways in nanothermites follow through the condensed state. Combust Flame 162:258–264. doi: 10.1016/j.combustflame.2014.07.002

34. Sullivan KT, Piekiel NW, Wu C, et al. (2012) Reactive sintering: An important component in the combustion of nanocomposite thermites. Combust Flame 159:2–15. doi: 10.1016/j.combustflame.2011.07.015

35. Chowdhury S, Sullivan K, Piekiel N, et al. (2010) Diffusive vs Explosive Reaction at the Nanoscale. J Phys Chem C 114:9191–9195. doi: 10.1021/jp906613p

36. Umbrajkar SM, Schoenitz M, Dreizin EL (2006) Exothermic reactions in Al–CuO nanocomposites. Thermochim Acta 451:34–43. doi: 10.1016/j.tca.2006.09.002

37. Dreizin EL, Schoenitz M (2015) Correlating ignition mechanisms of aluminum-based reactive materials with thermoanalytical measurements. Prog Energy Combust Sci 50:81–105. doi: 10.1016/j.pecs.2015.06.001

38. Mulamba O, Pantoya M (2014) Oxygen scavenging enhances exothermic behavior of aluminum-fueled energetic composites. J Therm Anal Calorim 116:1133–1140. doi: 10.1007/s10973-013-3622-1

39. Marín L, Nanayakkara CE, Veyan J-F, et al. (2015) Enhancing the Reactivity of Al/CuO Nanolaminates by Cu Incorporation at the Interfaces. ACS Appl Mater Interfaces 150529075915001. doi: 10.1021/acsami.5b02653

40. Jayaraman S, Mann AB, Reiss M, et al. (2001) Numerical study of the effect of heat losses on self-propagating reactions in multilayer foils. Combust Flame 124:178–194. doi: 10.1016/S0010-2180(00)00192-9

41. Bray J (1990) Properties and Selection: Nonferrous Alloys and Special-Purpose Materials. ASM Handb., Vol 2. ASM International, pp 29–61

42. Housh S, Mikucki B, Stevenson A (1990) Properties and Selection: Nonferrous Alloys and Special-Purpose Materials. ASM Handb., Vol 2. ASM International, pp 480–516